Optimal application of triggers for the deformation of crash structures under axial compression with consideration of geometrical imperfections

Johannes Sperber[1]*, **Christopher Ortmann**[1], **Axel Schumacher**[2]

[1] *Volkswagen AG, Wolfsburg, Germany*
* *Corresponding author: johannes.sperber1@volkswagen.de*
[2] *Chair for Optimization of Mechanical Structures, University of Wuppertal, Wuppertal, Germany*

Abstract
Extruded profile structures are widely used as efficient energy absorbers in vehicle front and rear ends throughout the automotive industry. Especially for crash structures under axial compression the usage of physical trigger mechanisms is state of the art to robustly initiate and maintain the desired deformation modes. To simulate these axially loaded crash structures, imperfections are needed to avoid unrealistic deformation modes caused by an ideal finite element model. Furthermore stochastic imperfections can be used for robustness evaluations. Hence an automatic model creation process has been developed which allows an application of geometrical imperfections on any given extruded profile structure. This is done by extending GRAMB (GRAph based Mechanics Builder) which is part of the Graph and Heuristic based Topology Optimization (GHT). Furthermore a parametrized and graph related mesh modification and morphing process has been implemented, which allows the application of various physical triggers such as indents, cutouts and chamfers on profiles generated by GRAMB. The application of the physical triggers has been investigated in parameter optimizations for a longitudinal member in a front crash load case. The crashworthiness of the front end has been improved and the robustness of the optimal designs was investigated.
Keywords: *Topology optimization, crash load cases, profile structures, geometrical imperfections, triggers for crash structures*

1. Introduction

Throughout the automotive industry, extruded profile structures are broadly used as efficient energy absorbers in vehicle front and rear ends. Although a lot of theoretical, experimental and numerical investigations have been performed over the years, there is still research work ongoing, particularly when it comes to the (topology) optimization of these structures in highly non-linear crash load cases (e.g. [1], [2]).
The present work is intended as a basis for a topology optimization of axially loaded structures with the Graph and Heuristic based Topology Optimization (GHT) [3]. Therefore the state of the art in the automotive industry such as the usage of physical triggers for the robust initiation and maintenance of desired deformation modes and crash characteristics has to be implemented in the automatic model creation process. Furthermore the simulation of these axially loaded crash structures requires the application of imperfections in order to avoid unrealistic deformation modes caused by an ideal FE model and to investigate the robustness regarding the structural response. Hence the GRAph based Mechanics Builder (GRAMB) which is part of the GHT is extended. GRAMB is used to extrude profile cross sections defined by a mathematical graph along a spline in order to automatically generate a finite element (FE) mesh. For the numerical studies in this work the explicit FE solver PAM-CRASH (v2017) is used.
In this work geometrical imperfections are defined as model modifications which are only used in FE simulation in order to acquire a better accordance with real world observations. In comparison, physical triggers are defined as imperfections that are utilized both on real world and simulation components to influence the crash characteristic of the component and to robustly establish and maintain a desired mode of deformation.

2. Geometrical imperfections

2.1 Background

For the progressive buckling of square profiles four types of modes are described by [4]: extensional, symmetric and two

asymmetric modes. The extensional mode (axis symmetric folding pattern – compare Fig. 1) absorbs more energy than the other modes, but it can barely be observed in real world tests. Instead the other three modes predominate. The simulation of the buckling behavior of straight profiles is challenging since small variations in boundary conditions, material properties and geometry can lead to a considerable variation in the structural behavior and therefore the energy absorption [5]. The ideal geometry description as well as ideal material data and ideal boundary conditions, which are usually used in FE simulation, often lead to extensional modes for squared tubes [6].

To get more realistic modes in the FE simulation, several measures can be taken. Most of these replicate imperfections found in real world specimens and test procedures: Stochastic material data [7], stochastic loading conditions, stochastic wall thickness distributions [7] or stochastic profile wall deflections (nodal displacements) [5][8]. Another measure often taken is the use of deterministic triggers (e.g. wall deflection at the top section of the profile) to enforce a profile collapse in the desired mode [9].

Since the method described in this paper should be used with any profile cross section topology created by GRAMB, where the desired mode is often unknown, a deterministic trigger for a specific mode is not an option. Furthermore since only the profile models themselves can be manipulated by GRAMB, stochastic loading or boundary conditions are unsuitable as well. [6] found that the deflection of the profile walls has the greatest influence on the crushing mode compared to wall thickness and wall length deviation. Therefore a stochastic modification based on wall deflection was found to suit the requirements best to enable realistic modes and robustness investigations for unknown profile cross sections in an automatic model creation process.

2.2 Simulation and application of stochastic fields

The approach for generating the stochastic fields used by [5] and [7] is based on research by [10] where methods for the simulation of multi-dimensional Gaussian stochastic fields by spectral representation are described. While [5] and [7] use a two dimensional, univariate Gaussian field (2D-1V) for their respective work, a new approach is described in this work which is applicable to generate smooth fields for more complex profile structures (e.g. with inner profile knots and walls) as well as an implementation in the automatic model creation process with GRAMB. The first term in "XD-YV" represents the input of the stochastic field (e.g. 2D or 3D FE node coordinates), while the second term describes the number of stochastic field output variables (1V – univariate).

For this purpose, two 3D-1V fields as described in [10] are used. The output of each field is used for the nodal displacement in both directions (x_1 and x_2) of the cross section plane respectively (Fig. 1). They are computed by a series of cosines (Eq. 1), which is computationally expensive but provides flexibility with non-equidistant meshes. For Eq. 1, random numbers (Φ_{n1n2n3}) between 0 and 1 have to be generated. Further information regarding Eq. 1 can be found in [10]. The simulation of the stochastic fields mathematically requires an infinite series of cosines. Since this cannot be established in an automated process which pursues short calculation times, a tradeoff has to be accepted and the number of sums is limited to a finite value (N_1=N_2=N_3=25).

$$f^{(i)}(x_1,x_2,x_3) = \sqrt{2}\sum_{n_1=0}^{N_1-1}\sum_{n_2=0}^{N_2-1}\sum_{n_3=0}^{N_3-1}\Big[A^{(1)}_{n_1n_2n_3}\cos\left(\kappa_{1n_1}x_1+\kappa_{2n_2}x_2+\kappa_{3n_3}x_3+\phi^{(1)(i)}_{n_1n_2n_3}\right)+A^{(2)}_{n_1n_2n_3}\cos\left(\kappa_{1n_1}x_1+\kappa_{2n_2}x_2+\kappa_{3n_3}x_3+\phi^{(2)(i)}_{n_1n_2n_3}\right)+ A^{(3)}_{n_1n_2n_3}\cos\left(\kappa_{1n_1}x_1+\kappa_{2n_2}x_2+\kappa_{3n_3}x_3+\phi^{(3)(i)}_{n_1n_2n_3}\right)+A^{(4)}_{n_1n_2n_3}\cos\left(\kappa_{1n_1}x_1+\kappa_{2n_2}x_2+\kappa_{3n_3}x_3+\phi^{(4)(i)}_{n_1n_2n_3}\right)\Big] \quad (1)$$

A power spectral density (PSD) function for 3D-1V fields is described in [11]. This function is part of the four A_{n1n2n3} terms in Eq. 1. As a tradeoff for the number of sums has to be accepted, the PSD function is modified in a way, that the output standard deviation of the stochastic fields corresponds with the input standard deviation.

$$S_{ff}(\kappa_1,\kappa_2,\kappa_3) = \sigma_f^2\,\frac{b_1b_2b_3}{16\pi}\;exp\left[-\left(\frac{b_1\kappa_1}{2}\right)^2-\left(\frac{b_2\kappa_2}{2}\right)^2-\left(\frac{b_3\kappa_3}{2}\right)^2\right] \quad (2)$$

The PSD function used is stated in Eq. 1, where σ_f is the standard deviation of the stochastic field. The parameters b_1, b_2 and b_3 are proportional to the correlation length of the stochastic fields in respective x_1-, x_2- and x_3-directions (Fig. 1). Since x_1 and x_2 are directed in the cross section plane, the same parameter $b_{profile}$ is used for b_1 and b_2. The parameter b_3 in extrusion direction is renamed to b_{ext}. The output values of both fields are calculated with Eq. 1, where the first field provides the stochastic displacement in x_1-direction, and the second field the ones in x_2-direction respectively. The input values for the simulation of both stochastic fields are the three dimensional FE node coordinates in the x_1-x_2-x_3 coordinate system. In this work the parameters described by [12] are used (Table 1).

Table 1. Parameters of the power spectral density function for local imperfections based on [12]

Imperfection	σ_f in mm	$b_{profile}$ in mm	b_{ext} in mm
Local	0.07	40	400

The method developed in this work can also be applied to profiles extruded along a three-dimensional spline. The x_1-x_2-x_3 coordinate system is therefore translated and rotated for each spline section so that the field is smoothly aligned throughout the whole extrusion length.

Fig. 1 shows example results for a square aluminum extrusion profile (AA6XXX T6, 80 x 80 x 400 mm, 1 kg) with and without applied stochastic fields in a simple drop hammer test. It can be seen that the dominant mode of deformation changed after the application of the stochastic fields from extensional mode to symmetric mode. For a series of ten test with individual stochastic fields an increase of 13.3% for the intrusion can be observed compared to the ideal FE geometry.

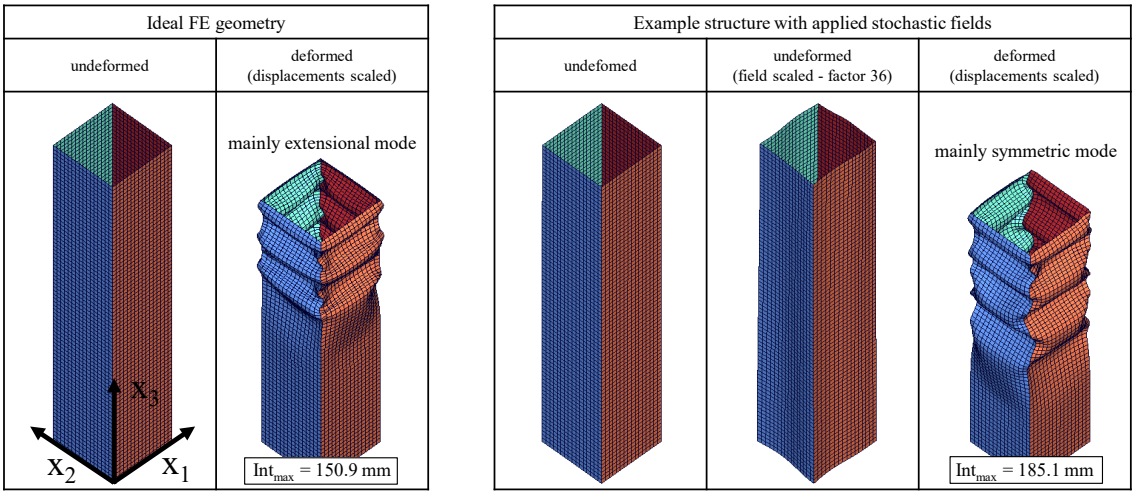

Figure 1. Application of stochastic fields on a squared single cell structure

3. Physical triggers

3.1 Background

Physical triggers are state of the art for automotive applications in order to initiate and maintain a defined and robust crash behavior. The topic has been studied intensively by many researchers. The work by [13] provides a broad overview over publications related to geometrical and material triggers for axially loaded crash structures. The measures described in literature contain prebuckling, corner indentations, triggering dents, corrugation of tubes, cutouts, chamfering, tube wrapping and many more.

Not all of the physical triggers listed above meet the requirements for an automotive application which seeks for cost efficient manufacturing while still being able to influence the crash characteristic significantly. As a result, indentations as well as various cutouts are the most common physical triggers for aluminum profiles in automotive front end applications. Hence these triggers are implemented in the automatic model creation process. Another trigger that seems industrially feasible is the chamfering of extruded profiles.

3.2 Modelling of physical triggers

The application of the physical triggers is implemented in the automatic model creation process with GRAMB as a downstream mesh modification and morphing process after the completion of the initial meshing. Own techniques were developed since a connection between the existing profile mesh geometry and the mathematical graph used by GRAMB should be established in order to integrate the physical triggers in the optimization process of the GHT. All triggers are defined by their relative position on the extrusion spline (from 0 to 1) and within the profile cross section as well as other trigger specific parameters such as the trigger dimensions. The triggers implemented are profile corner and wall indents, profile corner and wall cutouts as well as end- and mid-section chamfers. Example applications of the physical triggers

are illustrated in Fig. 2 (a). It should be noted that for the chamfering triggers not only the FE nodes are moved, but also the related element thicknesses are reduced. Fig. 2 (b) shows the specific modelling parameters for the wall indent trigger.

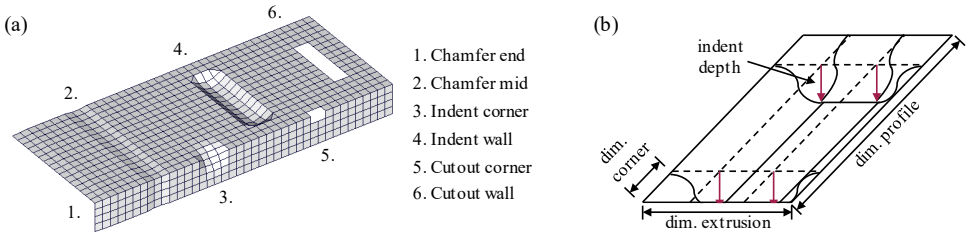

Figure 2. (a) Example application of physical triggers, (b) trigger specific parameters for wall indent trigger

4 Example optimization of triggers parameters in a crash load case

4.1 FE model

The crash test investigated in this work is the RCAR Front Impact [14]. In this load case a vehicle impacts at a speed of 15 km/h into an oblique (10°) rigid barrier with a 40% overlap. Instead of a full vehicle, a simple generic model of a vehicle front end is used (Fig. 3). It consists of an aluminum cross member facing the barrier with two aluminum longitudinal members tied to it. The material is AA6XXX T6 with a yield strength of 280 MPa.

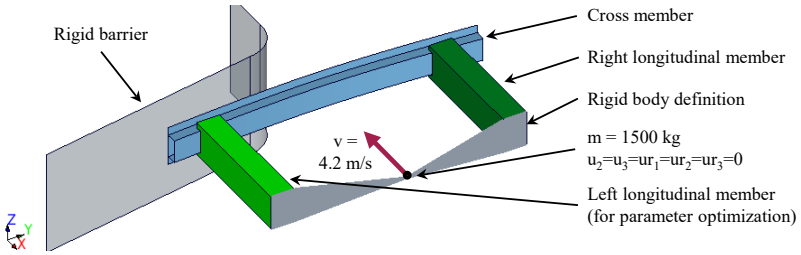

Figure 3. Example application of physical triggers

The longitudinal members are connected via a rigid body definition with a point mass which inherits the weight (1500 kg) and the initial velocity (15 km/h) of the vehicle. The longitudinal members have a length of 500 mm and a rectangular profile geometry (130 mm x 90 mm) with a wall thickness of 2 mm which is not changed during the optimizations. The triggers are only applied to the longitudinal member on the side of the barrier overlap.

4.2 Optimization setup

The parameter optimization is performed with GRAMB and the commercial software LS-Opt (v5.21). A genetic algorithm with direct optimization [15] is used for the present optimization problem since it provides good design space exploration which is needed for the highly nonlinear structural responses of the crash simulations. The design variables used for this optimization are the positions of the physical triggers in extrusion direction as described in section 3.2.

The objective of the optimization is the minimization of the maximum contact force measured between the front end and the barrier. Peaks in the force level during the crash event are undesirable since they can result in higher loads on the passengers as well as unwanted plastic deformation of downstream vehicle structures. As a constraint, the maximum intrusion is limited to 280 mm. To prevent the front end from sliding sideward along the barrier instead of absorbing energy by plastic deformation, a displacement constraint in y-direction is set.

4.3 Example parameter optimizations

In the first parameter optimization the position of twelve wall indents are used as design variables in order to trigger homogeneous symmetric buckling in the profile. In order to reduce the number of independent design variables, the position of the first trigger is used as one independent variable. As a second independent design variable a factor for the distances between the triggers is defined. Each trigger has a counterpart on the opposite profile side and the indent trigger positions on the long and short sides are shifted against each other in order to trigger the symmetric mode.

In the second parameter optimization four cutout triggers are applied to the structure. One cutout trigger is placed at each wall of the longitudinal member. The four axial positions of the triggers are the independent variables in this optimization. This optimization setup enables asymmetric trigger patterns, although the cutout triggers have corresponding positions close to cross member in the initial design.

The optimal designs found in each of the parameter optimizations and their structural responses are shown in Table 2 and Fig. 4. Both optimizations result in a more uniform and therefore improved force-displacement curve. In comparison, the force-displacement curve of the reference structure as well as the initial designs with triggers (not shown in Fig. 4) show high force amplitudes with significant decreases of the force level in between. The reference structure buckles with an asymmetric folding pattern in the beginning which then shifts to a more symmetric one in the consecutive folds.

Table 2. Results of the parameter optimization

Design	F_{max} in kN		Int_{max} in mm	
	initial	optimum	initial	optimum
Reference w/o trigger	71.9	-	275.5	-
Indent wall - 2 indep., 11 dep. design variables	83.4	57.9	239.7	272.6
Cutout wall - 4 indep. design variables	78.5	57.6	241.6	264.6

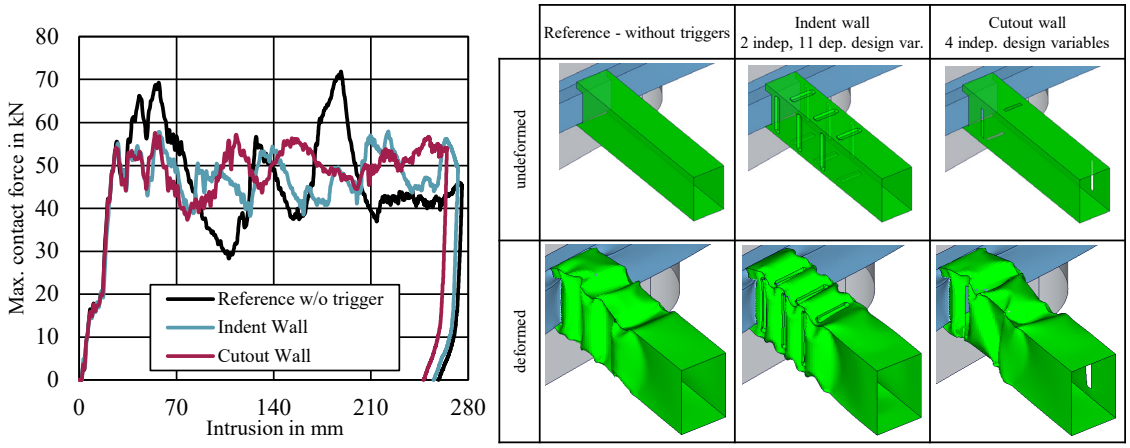

Figure 4. Reference and optimal designs from parameter optimization (displacement scaled with factor 0.5)

As intended by the optimization setup, the optimal structures with symmetric wall indents buckle in an almost perfect symmetric mode starting from the first fold on. The trigger setup lowers the force peaks significantly by directly initiating buckling in a symmetric mode and enforcing a shorter and therefore more efficient folding wavelength than in the reference structure. The symmetric buckling mode is maintained during the whole deformation. In comparison with the initial design, especially the distance between the trigger positions was increased (indent triggers in the initial design were more packed) in order to buckle in the symmetric folding pattern throughout the whole crash event.

For the optimization run with the cutout triggers at each side of the profile an asymmetric trigger pattern is the optimal design in terms of the achieved objective function. In contrast to the optimal symmetric wall indent design as well as to the reference design, the folding pattern observed here is more irregular. Still it results in a significant decrease of the maximum force comparable to the symmetric design. The first fold is initiated by two cutouts which reduce the first force peak effectively and induce an asymmetric pattern. A third cutout initiates the next fold which preserves the asymmetric behavior. The fourth cutout at the end of the profile is not utilized as a buckling initiator.

4.4 Robustness analysis of optimal designs

Although both trigger designs initiate completely different folding patterns, the resulting force reduction is still similar. To investigate the robustness of these designs, ten calculations per design with applied stochastic fields (section 2.2) are performed. The standard deviations for the maximum force and intrusion are used as an evaluation criteria for the robustness. Table 3 shows the results of this investigation. As expected, the design with the symmetric trigger pattern on its walls shows a more robust behavior regarding geometrical imperfections than the reference design and the design with

the asymmetric pattern. In case of the symmetric design the defined folding pattern induced by the numerus wall indents is the cause. For the cutout trigger design only the first two lobes are directly triggered by cutouts. Therefore no defined folding pattern is enforced for the consecutive folds. It even shows a less robust behavior than the reference design without any triggers. Due to the applied imperfections, a bifurcation point can be identified in the folding pattern of the cutout design and therefore also in the structural responses. It is caused by the asymmetric trigger pattern, the inferior number of triggers compared to the symmetric design as well as potential contact points at the cutout edges.

Table 3. Robustness of the optimal designs

Design	F_{max} in kN		Int_{max} in mm	
	mean	std.dev.	mean	std.dev.
Reference w/o trigger	71.6	0.67	275.5	0.70
Indent wall - 2 indep., 11 dep. design variables	57.9	0.13	272.7	0.34
Cutout wall - 4 indep. design variables	61.9	3.75	269.9	3.56

5. Conclusions

In this work the necessary foundations for a topology optimization of axially loaded structures with the GHT have been presented. The investigations show that the developed geometrical imperfections provide reasonable results for triggering realistic deformation modes and have potential for the evaluation of the robustness of crash structures at the end of an optimization. Furthermore the physical triggers presented in this paper have been used in parameter optimizations and lead to significant improvements in the crashworthiness of a generic front end.

Further research will focus on the development of new heuristics for the GHT in order to perform topology optimizations of axially loaded crash structures. Besides the heuristics also the optimization process itself needs adaptation for the application and optimization of physical triggers as well as a possible downstream robustness analysis.

References

1. Duddeck F et al.. Topology optimization for crashworthiness of thin-walled structures under axial impact using hybrid cellular automata. Struct Multidisc Optim 54:415–428; 2016
2. Fang J et al. On design optimization for structural crashworthiness and its state of the art. Struct Multidisc Optim 55:1091-1119; 2017
3. Ortmann C, Schumacher A. Graph and heuristic based topology optimization of crash loaded structures. Journal of Structural and Multidisciplinary Optimization 47:839–854; 2013
4. Abramowicz W, Jones N. Dynamic Axial Crushing of Square Tubes. International Journal of Impact Engineering 2:179-208; 1984
5. Fyllingen Ø, Hopperstad O S, Langseth M. Stochastic simulations of squared aluminium tubes subjected to axial loading. International Journal of Impact Engineering 34:1619-1636; 2007
6. Xue L, Lin Z, Jiang Z. Effects of Initial Geometric Imperfections on Square Tube Collapse. 6th International LS-DYNA Conference; Detroit; 2000
7. Stefanou G, Papadrakakis M. Stochastic finite element analysis of shells with combined random material and geometric properties. Comput. Methods Appl. Mech. Engrg. 193:139-160; 2003
8. Schenk C A, Schuëller G I. Buckling analysis of cylindrical shells with random geometric imperfections. International Journal of Non-Linear Mechanics 38:1119-1132; 2003
9. Kim H-S. New extruded multi-cell aluminum profile for maximum crash energy absorption and weight efficiency - Thin-Walled Structures 40:311–327; 2002
10. Shinozuka M, Deodatis G. Simulation of multi-dimensional Gaussian stochastic fields by spectral representation. Appl. Mech. Rev 49(1), 29-53; 1996
11. Papadrakakis M, Kotsopulos A. Parallel solution methods for stochastic finite element analysis using Monte Carlo simulation. Comput. Methods Appl. Mech. Engrg. 168:305-320; 1999
12. Lönn D, Fyllingen Ø, Nilsson L. An approach to robust optimization of impact problems using random samples and meta modelling. International Journal of Impact Engineering 37:723-734; 2010
13. Yuen S, Nurick G N. The Energy-Absorbing Characteristics of Tubular Structures with geometric and material modifications: An overview. Applied Mechanics Reviews 61:020802; 2008
14. RCAR. RCAR Low-speed structural crash test protocol. Issue 2.3; October 2017
15. Stander N et al. LS-OPT User's Manual Version 5.2. Livermore Software Technology Corporation; 2015